Original Paper

Impacts of mantle-derived fluids on source-related biomarkers in crude oils: A case study from the Dongying Depression, eastern China

Ting Liang [a, b, *], Mei-Lin Jiao [a, b], Xin-Liang Ma [a, b], Liu-Ping Zhang [c]

[a] State Key Laboratory of Petroleum Resources and Prospecting, China University of Petroleum (Beijing), Beijing, 102249, China
[b] College of Geosciences, China University of Petroleum (Beijing), Beijing, 102249, China
[c] Key Laboratory of Petroleum Resource, Institute of Geology and Geophysics, Chinese Academy of Science, Beijing, 100029, China

ARTICLE INFO

ABSTRACT

Mantle-derived fluids can change the biomarker compositions in oil, with respect to abnormal thermal energy and volatiles input. Identification the reliable biomarkers for oil-source correlation is important in the regions that have been affected by mantle-derived fluids. In the Dongying Depression, deep faults, including Gaoqing-Pingnan Fault in the western part and the Shicun Fault in the southern part, have provided the avenues by which large volumes of mantle-derived fluids have entered this petroliferous depression. For the purpose of comparison, oil and accompanied gas were collected from the active zones with mantle-derived fluids activities, and the stable zones with little mantle-derived fluids. According to isotopic analyses (i.e., helium isotope, $\delta^{13}C_{CO2}$ and δ^2H_{CH4}), mantle-derived fluids in the north part of the Dongying Depression have more H_2 and less CO_2 than those in the south part. The correlations between source-related biomarkers in crude oils and isotopic compositions in the corresponding gases suggest that many biomarker parameters have lost their original signatures due to the abnormal thermal energy, and H_2 and/or CO_2 derived from the mantle-derived fluids. Pr/Ph, for example, can be modified by both thermal energy and H_2 from the mantle-derived fluids. Systematic increase or decrease in the gammacerane index, C_{24} tetracyclic/C_{26} tricyclic terpane and C_{21}/C_{23} tricyclic terpane may be indicative of the occurrence of abnormal thermal energy. C_{31}/C_{30} hopane, DBT/TF and DBF/TF, in contrast, may indicate the contribution of hydrogenation as opposed to that of CO_2 supply. The relative distributions of C_{27}, C_{28} and C_{29} $\alpha\alpha\alpha$ (20R) steranes are probably altered little by the mantle-derived fluids. Based on the ternary diagram of C_{27}, C_{28} and C_{29} steranes, the oil samples collected from the Dongying Depression were largely the mixtures derived from source rocks in lower layer of the Es_3 member and upper layer of the Es_4 member.

1. Introduction

Mantle-derived fluids that ascend via deep faults into sedimentary basins (e.g., King, 1986) have been widely documented (e.g., Jin et al., 2004; Hu et al., 2009; Zhang et al., 2009, 2011; Caracausi et al., 2013; Bigi et al., 2014; Palcsu et al., 2014; Liu et al., 2017, 2021; Wang et al., 2022). Mantle-derived fluids can carry effective heat and release gases, which are typically composed of CH_4, CO_2, N_2, and H_2, into the reservoirs (Caracausi et al., 2008, 2013; Nuccio et al., 2014; Liu et al., 2017, 2021; Wang et al., 2022;

Guan et al., 2023). These fluids, thus, can cause systematic changes in biomarker compositions with respect to the abnormal thermal energy and volatiles input. The thermal energy, for example, may cause thermal cracking of C−C bonds in high molecular weight components, and consequently affects the distribution patters of the biomarkers (Clifton et al., 1990; Zhao et al., 2005; Wang et al., 2006; Jin et al., 2007; Huang et al., 2016). Hydrogen gas, in contrast, could affect the distribution patters of *n*-alkanes and isoprenoids by hydrogenation (Jin et al., 2002, 2004, 2007), whereas mantle-derived CO_2 fluids can preferentially extract the lighter saturated hydrocarbons from oils (Liu et al., 2017). Therefore, the influence of mantle-derived fluids on biomarkers needs to be properly accounted for before oil-source correlations, which are largely based on biomarker fingerprints. However, previous studies

mostly focused on *n*-alkanes and isoprenoids. Little is known about the responses of many source-related biomarkers, including steranes, terpanes, and aromatics to mantle-derived fluids. Furthermore, many of the previous studies on the effects of mantle-derived fluids are based on experimental simulation of source rocks. It is uncertain that if mantle-derived fluids can alter biomarkers in crude oils similarly. As such, the effects of mantle-derived fluids on source-related biomarkers in crude oils have to be addressed.

The Dongying Depression is one of the most petroliferous-rich areas in the Bohai Bay Basin in eastern China (Fig. 1). There, mantle-derived fluids are found in the areas close to deep faults and/or with abundant igneous rocks (Jin et al., 2004). In contrast, other areas are relatively stable, with little if any, activity of mantle-derived fluids (Fig. 1). As such, the comparison between active and stable zones in the Dongying Depression allows an assessment of the role played by abnormal heat and gases released from mantle-derived fluids on the biomarkers in the crude oils. This study, therefore, will (1) evaluate the effect of thermal energy as opposed to that of H_2 and CO_2 on source-related biomarkers, and (2) suggest reliable source-related biomarkers, that appear to be immune to thermal energy, H_2 and/or CO_2 input.

2. Geological setting

2.1. Regional geology

The Bohai Bay Basin, which is a lacustrine basin located in eastern China, is bordered by the Tan-Lu Fault to the east, the Yanshan Orogen to the north, the Taihang Mountain to the west, and the Luxi Uplift to the south (Fig. 1(a)). The basin has undergone intense fault-block rifting and active magma movements since the late Mesozoic (Allen et al., 1997; Zhang, 1997). The Dongying Depression, with an area of 5700 km^2, is a half-graben developed in the south part of the Bohai Bay Basin. In this depression, the Gaoqing-Pingnan Fault in the western part and the Shicun Fault in the southern part are major deep faults (Jin et al., 2002; Fig. 1(b)). Tertiary volcanic rocks and CO_2 pools are located along these faults (Jin et al., 2002; Zhang et al., 2009; Fig. 1(b)), which provided pathways for mantle-derived fluids migrating into the depression (Liu et al., 1995).

The Paleogene strata in the Dongying Depression include the Kongdian Formation (Ek), the Shahejie Formation (Es) and the Dongying Formation (Ed). The Kongdian Formation, with a thickness of 0–2000 m, is a red bed succession consisting of coarse clastic rocks that unconformably overlies the Mesozoic basement. This formation is overlain by the Shahejie Formation and the Dongying Formation, which are the main oil and gas-bearing formations in the basin (Hu et al., 1989; Group of Shengli Oil Field Compiling Petroleum Geology, 1993). The Shahejie Formation is divided into four members, that are labelled, from oldest to youngest, as Es$_4$ (up to 1500 m thick), Es$_3$ (220–380 m thick), Es$_2$ (160–230 m thick) and Es$_1$ (120–195 m thick). Es$_4$ was deposited during the initial rifting stage, whereas Es$_3$ was deposited as syn-rift sediments (Hu et al., 1989; Group of Shengli Oil Field Compiling Petroleum Geology, 1993). Es$_4$ and Es$_3$ members are further divided into the upper (i.e., Es$_4^1$ and Es$_3^1$) and the lower layers (i.e., Es$_4^2$ and Es$_3^2$). Es$_4^1$ and Es$_3^2$, which typically consist of mudstones, shales and oil shales, and are the main source rocks in the Dongying Depression (Zhu et al., 2004a, 2004b). In Es$_4^1$, the total thickness of source rock is about 340 m, whereas in Es$_3^2$ it is up to 840 m thick (Pang et al., 2003). The sediments that now form the members Es$_2$ and Es$_1$ were deposited during a contraction of the lake. As such, the member Es$_2$ consists of intercalated purple and grey-green mudstones, sandstones, conglomerate, whereas member Es$_1$ is formed of gypsum-halite and/or sandstones. The Dongying Formation, 410–510 m thick, typically consists of fluvial and lacustrine grey mudstones and sandstones. The upper surface of the Dongying Formation is defined by an unconformity, which is overlain by the Neogene Guantao Formation (Ng, 250–300 m thick) and the Minghuazhen Formation (Nm, 700–760 m thick) (Hu et al., 1989; Group of Shengli Oil Field Compiling Petroleum Geology, 1993, Fig. 2).

2.2. Source rock geochemistry

Source rocks from Es$_4^1$ commonly has total organic carbon (TOC) greater than 1.1 wt%, with a maximum of 4.8 wt% (Hao, 2007). The kerogen types are I and II$_1$, with %R_o = 0.42–0.64 (Tan et al., 2002; Jiang et al., 2003; Yang and Zhang, 2008). This source rock, deposited in a shallow to semi-deep lacustrine and hypersaline environment (Zhu et al., 2004b; Hao, 2007). The TOC of the source rock from Es$_3^2$, in contrast, is typically between 2.0 and 5.0 wt% (Hao, 2007). It is dominated by type II$_1$ kerogen, with %R_o = 0.32–0.64 (Tan et al., 2002; Jiang et al., 2003; Yang and Zhang, 2008). The source rock from Es$_3^2$ formed in a deep lacustrine and semi-saline to fresh water environment (Zhu et al., 2004b).
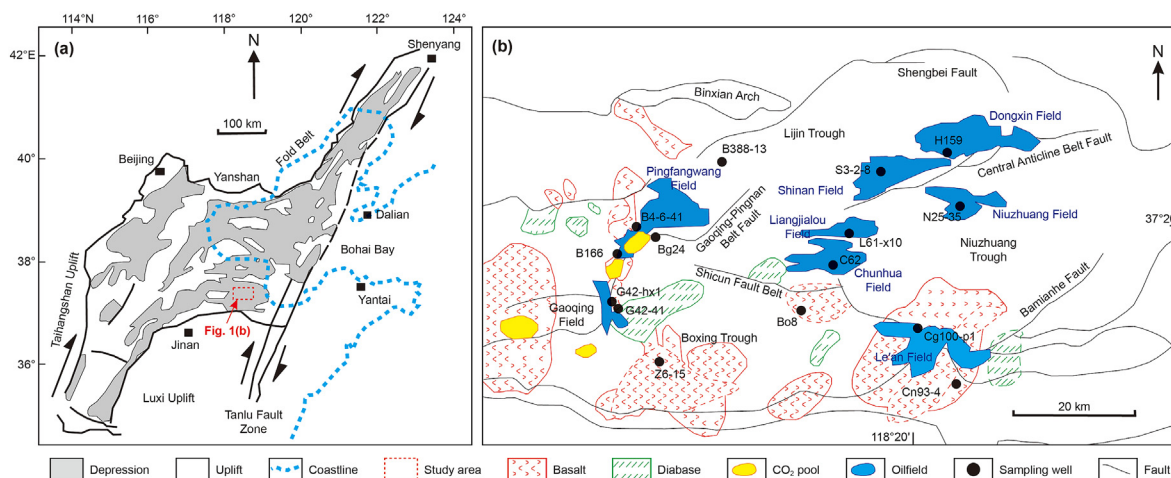

Fig. 1. Location map of the Dongying Depression. **(a)** Structural map of the Bohai Bay Basin and location of the Dongying Depression (modified from Li et al., 2024); **(b)** structural map of the Dongying Depression showing distribution of faults, CO_2 pools, igneous rocks and oilfields (modified from Zhang et al., 2009, and based on maps from Jin et al., 2002).
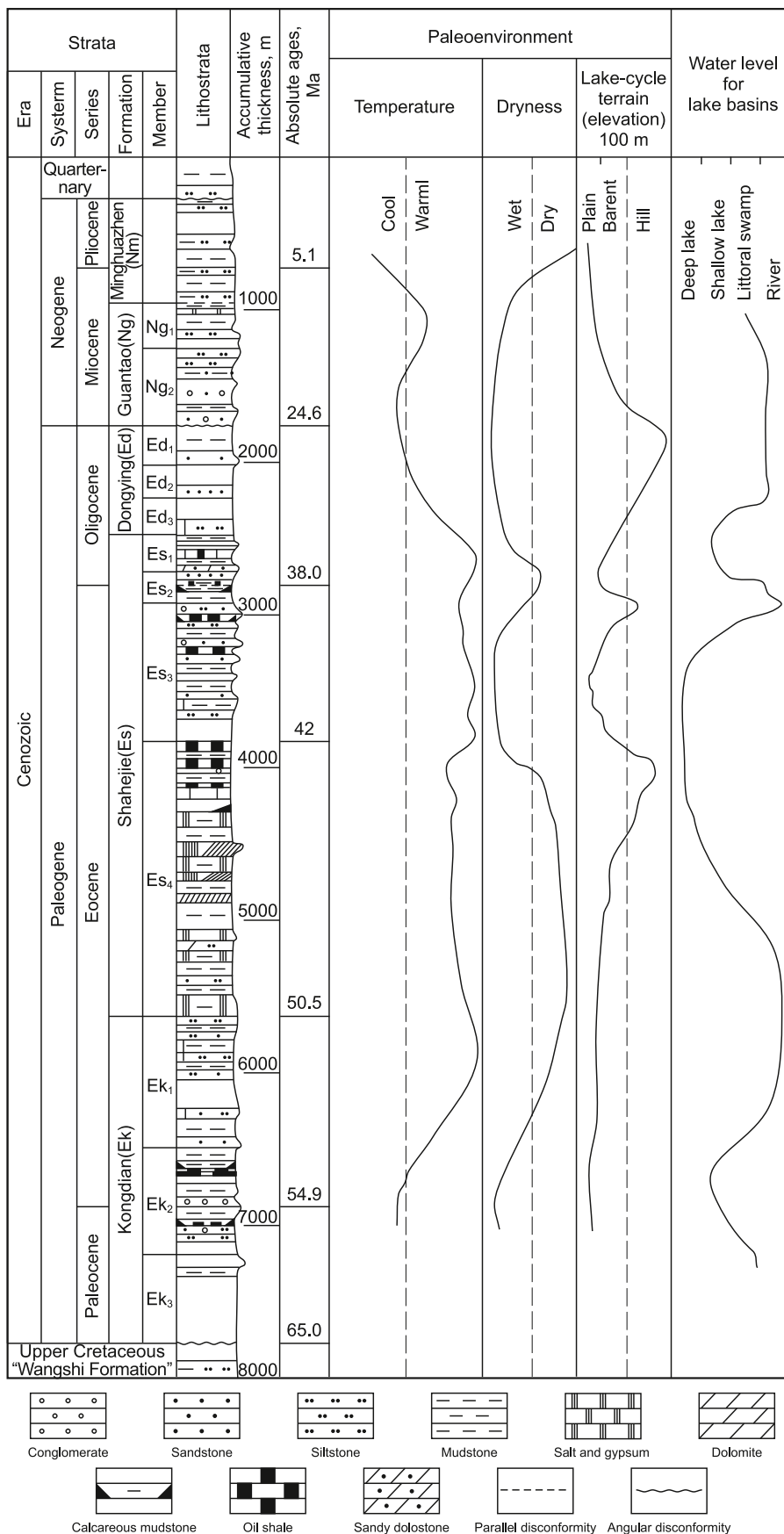
Fig. 2. Generalized Cenozoic stratigraphy of the Dongying Depression showing lithology and paleoenvironment of each unit (modified from Group of Shengli Oil Field Compiling Petroleum Geology, 1993).

3. Samples and methods

3.1. Samples

Oil and gas samples were collected in pairs from 18 production wells in the Dongying Depression (Fig. 1(b) and Table 1). For the purpose of comparison, thirteen wells were located in the zones with documented mantle-derived fluid activities (i.e., Gaoqing-Pingnan and Shicun Fault Belts) with burial depths of 863–3062 m, and the other five were from the stable zones with little, if any, mantle-derived fluids (i.e., Niuzhuang Trough) with a burial depth of 2600–3328 m (Fig. 1 and Table 1). Gas samples were collected directly from the wellheads or separators after flushing the lines for 2–3 min to remove air contamination. The collection of each gas sample used a stainless-steel cylinder (10 cm in diameter and 5000 cm^3 in volume), which is equipped with shut-off valves on both sides. A maximum pressure of 22.5 MPa was used to collect the gas samples. The pressure inside the container was kept higher than the atmospheric pressure. After collection, the bottles were immersed in a water bath to test for any leakage. The corresponding oil samples were collected from wellheads or separators in glass jars. Density, API and sulfur content of oil samples were provided by the Shengli Oilfield Company (Table 2).

3.2. Helium, hydrogen and carbon isotopes in gas

Isotopic compositions of the gas samples, including $^3He/^4He$, $\delta^{13}C_{CO2}$ and δ^2H_{CH4}, were obtained in this study (Table 1). Helium isotope ratios were determined by a MM5400 mass spectrometer at Lanzhou Center for Oil and Gas Resources, Chinese Academy of Sciences, with an analytical error of $\pm0.25\%$. The $^3He/^4He$ (i.e., R) of the gas samples were standardized against purified atmospheric helium (i.e., Ra = 1.4×10^{-6}).

Measurement of the carbon isotopic composition of CO_2 (i.e., $\delta^{13}C_{CO2}$) and CH_4 (i.e., $\delta^{13}C_{CH4}$), and hydrogen isotopic composition of CH_4 (i.e., δ^2H_{CH4}) were performed on a DELTAplus XP mass spectrometer at Lanzhou Center for Oil and Gas Resources of Chinese Academy of Sciences. The $\delta^{13}C_{CO2}$ and $\delta^{13}C_{CH4}$ values are reported relative to the Pee Dee Belemnite (PDB) standard in per mil (‰), whereas the δ^2H_{CH4} (i.e., δD_{CH4}) values are reported relative to Vienna Standard Mean Ocean Water (VSMOW) in per mil (‰). The errors associated with these results are $\pm0.3\%$ for $\delta^{13}C$ and $\pm0.05\%$ for δ^2H.

3.3. Gas-chromatography (GC) and GC-mass spectrometry (GC-MS) in oil

Eighteen crude oil samples were analyzed by GC for the normal alkane and acyclic isoprenoids, and by GC-MS for terpanes, steranes, hopanes and polycyclic aromatic hydrocarbons (PAHs). GC analyses were performed using an Agilent 6890 chromatography (fused silica column, 60 m × 0.25 mm × 0.25 μm) equipped with a flame ionization detector (FID). The oven temperature was initially held at 100 °C for 1 min, programmed to 300 °C at 3 °C/min and held at 300 °C for 20 min. The GC-MS of the saturated and aromatic hydrocarbon fractions were carried out on an Agilent 6890 gas chromatograph coupled to an Agilent 5975 mass selective detector (MSD). A HP-5MS fused silica column (60 m × 0.25 mm × 0.25 μm) was used. The carrier gas was helium, with a constant flow rate of 1 mL/min. For analyzing saturated hydrocarbon fraction, the GC oven temperature was programmed from 100 to 325 °C at 3 °C/min, with the initial and final hold times of 2 and 20 min, respectively. For the aromatic hydrocarbon fraction, the GC oven was programmed from 80 °C (1 min) to 320 °C at 3 °C/min, and held at 320 °C for 10 min. The mass spectrometer was operated in selected

ion monitoring (SIM) mode. Internal standards, d4 C_{29} 20R and d8 dibenzothiophene, were added to the oil samples for quantification of saturated and aromatic hydrocarbon fraction. Concentrations and biomarker parameters were calculated from peak area.

3.4. Degrees of correlation

In this study, correlations were made between source-related biomarker parameters in oil samples and isotopes in their accompanied gas samples. Pearson correlation coefficients were used to quantitatively evaluate the strength of each linear relationship, whereas p-values were used to estimate the probability of no correlation. Typically, a p-value less than 0.05 was regarded as statistically significant (Fisher, 1992; Xu et al., 2023). As such, a Pearson correlation coefficient within [−1, −0.6] or [0.6, 1], together with a p-value <0.05, reflects a correlation between X and Y. Otherwise, the X and Y are considered to be independent with each other.

4. Results

4.1. Helium, hydrogen and carbon isotopes in gas

In the Dongying Depression, the R/Ra ratios in the active zones range from 0.4 to 3.6, with most greater than 1.0. In contrast, in the stable zones, the R/Ra ratio is 0.1−0.4 (Table 1). The δ^2H_{CH4} values in the active zones have a large variation between −274.0‰ and −53.1‰, whereas those in the stable zones range are from −145.4‰ to −108.5‰ (Table 1). The δ^2H_{CH4} values, which are greater than −100‰, are obtained in the gases from the Gaoqing-Pingnan (e.g., Samples B4-6-41 and B338-13) and Shicun Deep Fault Belts (e.g., Sample Cn93-4), with the largest value up to −53.1‰ (Table 1). The $\delta^{13}C_{CH4}$ values range between −58.9‰ and −43.9‰ in the active zones, whereas those in the stable zones vary between −55.8‰ and −52.5‰ (Fig. 3(a)). The $\delta^{13}C_{CO2}$ values in the active zones (−15.7‰–6.4‰) are generally more positive than those in the stable zones (−14.3‰ to −7.5‰). A negative covariance exists between δ^2H_{CH4} and $\delta^{13}C_{CO2}$ (Fig. 3(b)), whereas there is no obvious correlation between R/Ra and δ^2H_{CH4} or $\delta^{13}C_{CO2}$ (Fig. 3(c) and (d)).

4.2. Biomarkers in crude oil

4.2.1. N-alkanes and isoprenoids

In the stable zones, $\Sigma nC_{21-}/\Sigma nC_{22+}$ varies from 1.0 to 1.4, whereas this ratio in the active zones ranges from 0.4 to 3.0 (Figs. 4 and 5(a)–(c)). Although the $\Sigma nC_{21-}/\Sigma nC_{22+}$ values are poorly correlated with R/Ra and δ^2H_{CH4}, they are negatively correlated with $\delta^{13}C_{CO2}$ (Fig. 5(a)–(c)).

The Pr/Ph ratio in the stable zones is relatively low (0.47−0.84), whereas that in the active zones varies from 0.37 to 1.41 (Fig. 5(d)−(f) and Table 3). In general, the Pr/Ph values are poorly correlated with R/Ra, δ^2H_{CH4}, and $\delta^{13}C_{CO2}$ values (Fig. 5(d)−(f)).

4.2.2. Steranes and terpanes

Sterane (m/z 217) mass chromatograms of representative oil samples are shown in Fig. 6. In the study area, the relative abundances of C_{27}, C_{28} and C_{29} ααα (20R) steranes (i.e., $C_{27}/\Sigma C_{27-29}$, $C_{28}/\Sigma C_{27-29}$, $C_{29}/\Sigma C_{27-29}$) fall within the ranges of 0.24−0.62, 0.21−0.31, and 0.26−0.53, respectively, with little differences between the stable and active zones (Fig. 7). All of these parameters are poorly correlated with R/Ra, δ^2H_{CH4} and $\delta^{13}C_{CO2}$ (Supplementary Fig. S1).

Representative mass chromatograms of m/z 191 are shown in Fig. 8. In the study area, the gammacerane index is commonly low. In the oil samples from the stable zones, for example, the

Table 1
Isotopic compositions of gas in the Dongying Depression, eastern China.

Magnitude of Mantle-derived fluid	Structure Location	Sampled Wells	Strata	Depth below sea level, m	R/Ra	$\delta^{13}C_{CO2}$	δ^2H_{CH4}	$\delta^{13}C_{CH4}$
Active zones	Gaoqing- Pingnan Fault Belt	G42-hx1	Ek	1080−1375	1.73	−4.4	−212.0	−46.3
		G42-41	Ek	980−1000	1.58	2.1	−215.0	−44.3
		B166	O	2425−2455	3.34	−9.9	−119.2	−47.5
		Bg24	O	2404−2410	3.64	−6.2	−184.7	−47.8
		B4-6-41	Es_4	1535−1569	3.04	−9.3	−80.9	−48.9
		B338-13	Es_3	1735−1738	0.79	n.d.	−53.1	−58.9
	Shicun Fault Belt	B8	Es_4	2650−2668	0.61	−5.7	−255.0	−51.9
		C13-404	Es_3+Es_4	1217−1315	0.42	5.2	−205.0	−45.1
		C62	Es_3	1260−1268	0.58	6.4	−218.0	−44.3
		Cg100-p1	O	863−1010	0.45	−2.7	−101.7	−46.1
		Cn93-4	O	900−907	1.21	−15.7	−68.3	−48.38
	Boxing Through	F143-5	Es_4	3009−3062	1.98	−5.4	−274	−48.0
		Z6-15	Es_1	1588−1895	0.52	−1.7	−235	−49.3
Stable zones	Central Anticline Belt	S3-2-8	Es_3	3307−3328	0.21	−10.7	−142.6	−52.5
		H159	Es_3	2946−2966	0.09	−14.3	−108.5	−55.8
	Niuzhuang Trough	N25-35	Es_3	3256−3271	0.08	−8.5	−119.1	−55.0
		L61-x10	Es_3	3281−3341	0.14	−7.5	−145.4	−53.7
		C26-21	Es_4	2600−2604	0.35	n.d.	n.d.	−56.0

Notes: The $^3He/^4He$ isotope ratio is expressed as R/Ra, where R= $(^3He/^4He)_{sample}$ and Ra= $(^3He/^4He)_{atm}$ = 1.400E-6; n.d. = no data; R/Ra and $\delta^{13}C_{CO2}$ data for B166, Bg 24, B4-6-1, B338-13, Cg100-p1, Cn93−4, S3-2-8, H159, N25−35, L61-x10, and C26-21 first reported by Zhang et al. (2011).

Table 2
Density and sulfur content of crude oils in the Dongying Depression.

Magnitude of Mantle-derived fluid	Structure Location	Sampled Wells	Strata	Depth below sea level, m	Specific gravity, g/cm³	API, °	Sulfur content, ppm
Active zones	Gaoqing- Pingnan Fault Belt	G42-hx1	Ek	1080−1375	n.d.	n.d.	n.d.
		G42-41	Ek	980−1000	n.d.	n.d.	n.d.
		B166	O	2425−2455	0.8580	33.42	0.23
		Bg24	O	2404−2410	0.8783	29.61	n.d.
		B4-6-41	Es_4	1535−1569	0.8786	29.55	n.d.
		B338-13	Es_3	1735−1738	n.d.	n.d.	n.d.
	Shicun Fault Belt	B8	Es_4	2650−2668	n.d.	n.d.	n.d.
		C13-404	Es_3+Es_4	1217−1315	n.d.	n.d.	n.d.
		C62	Es_3	1260−1268	n.d.	n.d.	n.d.
		Cg100-p1	O	863−1010	0.9859	12.02	1.76
		Cn93-4	O	900−907	n.d.	n.d.	n.d.
	Boxing Through	F143-5	Es_4	3009−3062	n.d.	n.d.	n.d.
		Z6-15	Es_1	1588−1895	n.d.	n.d.	n.d.
Stable zones	Central Anticline Belt	S3-2-8	Es_3	3307−3328	0.8728	30.62	0.08
		H159	Es_3	2946−2966	0.9	25.72	0.96
	Niuzhuang Trough	N25-35	Es_3	3256−3271	0.8903	27.44	0.66
		L61-x10	Es_3	3281−3341	0.8603	32.98	n.d.
		C26-21	Es_4	2600−2604	0.8880	27.85	1.01

gammacerane index varies from 0.07 to 0.48, whereas in the active zones the range is from 0.10 to 0.58 (Fig. 5(g)−(i) and Table 3). In addition, a negative covariance exists between the gammacerane index and R/Ra (Fig. 5(g)) in the samples from active zones, whereas δ^2H_{CH4} (Fig. 5(h)) and $\delta^{13}C_{CO2}$ (Fig. 5(i)) are not correlated with the gammacerane index.

The C_{31}/C_{30} hopane, defined as the ratio of C_{31} 22R homohopane/C_{30} hopane, is slightly larger in the active zones than that in the stable zones. In the stable zones, for example, C_{31}/C_{30} hopane varies from 0.37 to 0.46, whereas that in the active zones range from 0.37 to 0.63. Additionally, the ratio of the C_{31}/C_{30} hopane is negatively correlated with δ^2H_{CH4} (Fig. 9(b)), but positively correlated with $\delta^{13}C_{CO2}$ (Fig. 9(c)). In contrast, there is no covariance between C_{31}/C_{30} hopane and R/Ra (Fig. 9(a)).

In the stable zones, C_{24} tetracyclic/C_{26} tricylic terpane and C_{21}/C_{23} tricylic terpane are 0.33−0.40 and 0.64−0.79, respectively. Compared to those in the stable zones, C_{24} tetracyclic/C_{26} tricylic terpane and C_{21}/C_{23} tricylic terpane in the active zones, have larger ranges with the former varying from 0.28 to 0.57 and the latter from 0.62 to 1.08. A negative covariance exists between C_{24} tetracyclic/C_{26} tricylic terpane and R/Ra in the samples from active zones (Fig. 9(d)). The δ^2H_{CH4} (Fig. 9(e)) and $\delta^{13}C_{CO2}$ values (Fig. 9(f)), in

contrast, are generally not correlated with C_{24} tetracyclic/C_{26} tricylic terpane. For C_{21}/C_{23} tricylic terpane, although this ratio in the active zones is slightly higher than that in the stable zones, it is lack of any positive covariance between C_{21}/C_{23} tricylic terpane and R/Ra in the active zones (Fig. 9(g)). Furthermore, C_{21}/C_{23} tricylic terpane changes little with increasing δ^2H_{CH4} and $\delta^{13}C_{CO2}$ values (Fig. 9(h) and (i)).

4.2.3. Three fluorene series compounds (TF)

TF include dibenzothiophene (DBT), dibenzofuran (DBF) and fluorine (F). In the study area, the relative abundance of DBT is much higher than that of DBF. The DBT/TF ratios range from 0.14 to 1.00 in the active zones and from 0.78 to 0.90 in the stable zones (Table 3). DBF, in contrast, is partly below the detective limit. There are only seven oil samples from the active zones that show trace amount of DBF, with the DBF/TF ratio varying from 0.08 to 0.33 (Table 3). Additionally, the DBT/TF values are positively correlated with δ^2H_{CH4} and negatively correlated with $\delta^{13}C_{CO2}$, but lack any correlation with R/Ra (Supplementary Fig. S2(a)−(c)). In contrast, the covariance between DBF/TF and R/Ra (or δ^2H_{CH4}, or $\delta^{13}C_{CO2}$) is not evident (Supplementary Fig. S2(d)−(f)).
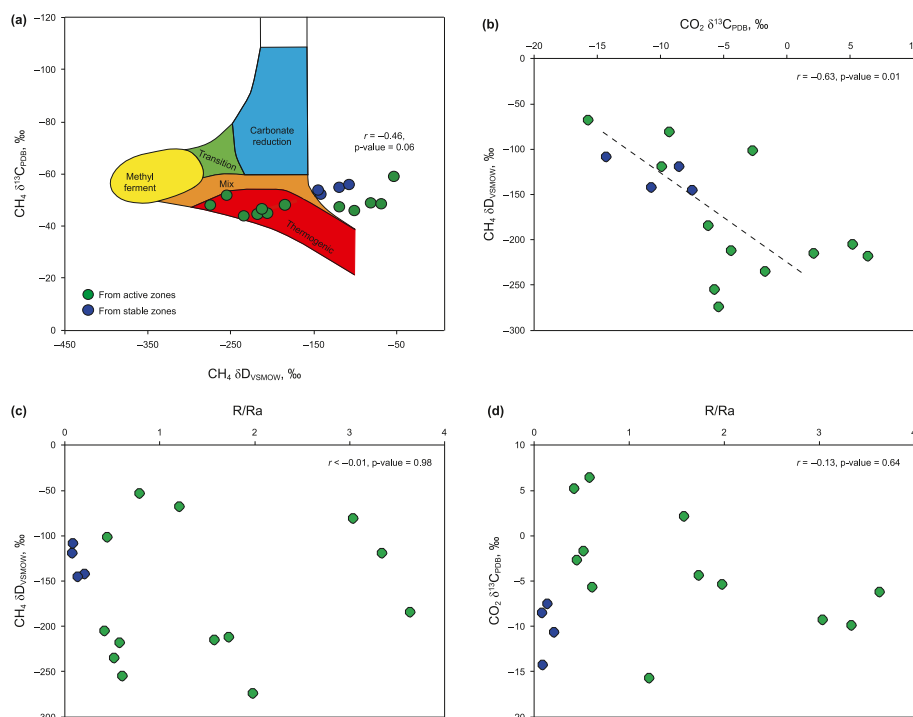
Fig. 3. Correlation diagrams **(a)** between δD_{CH4} and $\delta^{13}C_{CH4}$, **(b)** between δD_{CH4} and $\delta^{13}C_{CO2}$, **(c)** between δD_{CH4} and R/Ra, and **(d)** between $\delta^{13}C_{CO2}$ and R/Ra in gas from the Dongying Depression. The isotopic compositions for different types of methane in (a) are modified from Whiticar (1990). "*r*" is short for Pearson correlation coefficient.

5. Discussion

5.1. Occurrence of mantle-derived fluids

Deep faults provide migration pathways for mantle-derived fluids (Liu et al., 1995). In the study area, the Gaoqing-Pingnan and Shicun Fault Belts are such structures. Movement of the Gaoqing-Pingnan Belt probably took place between the Middle Jurassic and Pliocene (Shen et al., 2007), whereas that of the Shicun Fault Belt is poorly understood. The migration of mantle-derived fluids along the Gaoqing-Pingnan and Shicun Fault Belts is evident from the (1) Tertiary igneous rocks found along these zones (Liu et al., 1995); (2) high values of helium isotopes in the natural gas reservoirs (Liu et al., 1995); (3) mantle-derived CO_2 pools found in these fault belts (Zhang et al., 2011); and (4) the accumulation of hydrothermal alkanes in these two belts (Jin et al., 2002).

Given that the $^3He/^4He$ ratio in the mantle is approximately three orders of magnitude higher than those produced in the crust (R/Ra in crust is 0.01−0.1), the R/Ra ratio has commonly been used to evaluate the gas contributions from the mantle (Xu, 1996; Dai et al., 2009; Zhang et al., 2009). The variation of R/Ra in the Dongying Depression, therefore, indicates that (1) the flux intensities of mantle-derived fluids in the active zones are locally heterogeneous, and (2) the contributions of mantle-derived fluids in the stable areas are much less than those in the active zones. Given (1) the mantle-derived fluids are the heat carriers, and (2) the helium isotopes may quantitatively reflect the contribution from mantle, the R/Ra can be used as an indicator of the contribution of thermal energy from mantle-derived fluids.

Typically, δ^2H_{CH4} value in the wet gas varies from −260‰ to −150‰, whereas that in the dry gas ranges from −180‰ to −130‰ (Schoell, 1980). Compared with that organic methane, thermogenic methane commonly has more positive δ^2H values (Fig. 3(a); Whiticar, 1990). δ^2H_{CH4} values of geothermal gases in New Zealand, for example, range from −197‰ to −142‰ (Lyon and

Hulston, 1984) and −135‰ to −122‰ (Botz et al., 2002). Moreover, hydrogen gas derived from mantle favors the hydrogenation of organic matter, which produces methane high in δ^2H (Jin et al., 2002, 2007). This study illustrates that δ^2H_{CH4} and $\delta^{13}C_{CH4}$ are mostly compatible with the range of thermogenic methane (Fig. 3(a)). For $\delta^{13}C_{CO2}$, previous studies demonstrated that the $\delta^{13}C_{CO2}$ values increased with an increase in the content of mantle-derived CO_2 (Jin et al., 2002, 2007; Zhang et al., 2011). Therefore, the amount of H_2 and CO_2 derived from mantle-derived fluids are positively proportional to the δ^2H_{CH4} and $\delta^{13}C_{CO2}$ values in the gas, respectively (Jin et al., 2002, 2007; Zhang et al., 2009, 2011).

In the Dongying Depression, the δ^2H_{CH4} values are negatively correlated with $\delta^{13}C_{CO2}$ (Fig. 3(b)), indicating the amount of H_2 in the mantle-derived fluids may decrease as the amount of CO_2 increases. In general, the mantle-derived fluids in the north part of the Dongying Depression are relatively H_2-rich, whereas those in the south part are relatively CO_2-rich. This is consistent with the suggestion of Jin et al. (2004). In contrast, the lack of correlation between the R/Ra and δ^2H_{CH4} (or $\delta^{13}C_{CO2}$) (Fig. 3(c) and (d)), indicates that the thermal energy is not proportional to the gases released from the mantle-derived fluids.

5.2. Influence of biodegradation

The influences of biodegradation and mantle-derived fluids on the distribution of source-related biomarkers cannot be differentiated unambiguously. In the Dongying Depression, biodegradation has been widely documented in the Le'an oil field (e.g., Zhang et al., 2009; Niu et al., 2022). Indeed, this study shows that the oil from the Le'an oil field, including Cg100-p1, Cn93−4 and C62, appear to have suffered moderate to severe biodegradation, because (1) oils in Cg100-p1, Cn93−4 and C62 are heavy oils, characterized by low API gravity (<13°) and high sulfur content (>1.6 ppm) (Zhang et al., 2009), (2) an unresolved complex mixture (UCM) occurs, with partial removals of *n*-alkanes (Fig. 4(g) and (h)), and (3) the
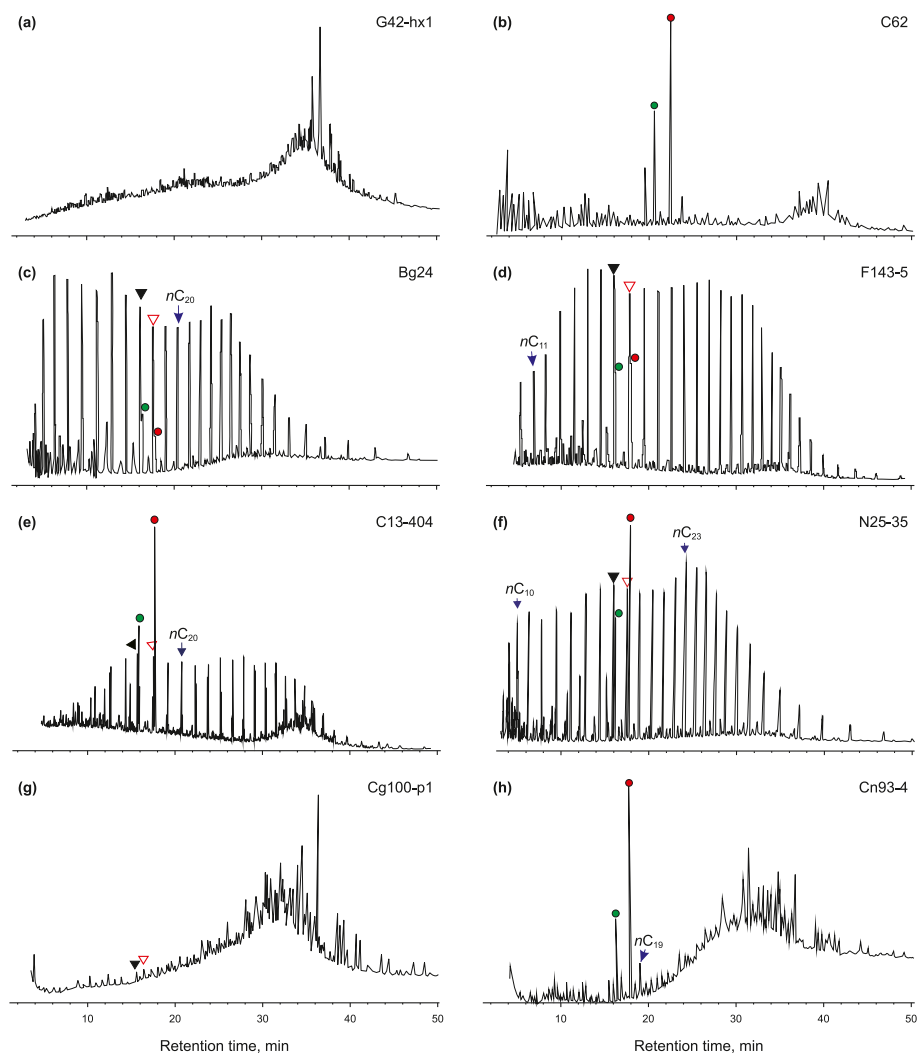
Fig. 4. Gas chromatograms of representative crude oils from the Dongying Depression. The peak labels denote the carbon number of *n*-alkanes; green circle denotes Pr; red circle denotes Ph; red triangle denotes *n*-C$_{18}$; black triangle denotes *n*-C$_{17}$.

appearance of C$_{29}$ 25-norhopane (Fig. 8). Moreover, the absence of *n*-alkanes and the abundance of C$_{29}$ 25-norhopane in G42-hx1 and G42-41 indicates a more advanced biodegradation than Cg100-p1, Cn93−4 and C62 (Figs. 4 and 8). Other oil samples, in contrast, show medium-high API gravity (25−38°), low sulfur contents (0.08−1.01 ppm), complete *n*-alkanes and absence of C$_{29}$ 25-norhopane, that indicate minimal levels of biodegradation. Although oils collected from Cg100-p1, Cn93−4, C62, G42-hx1 and G42−41 may have suffered biodegraded, the systematic changes of biomarker parameters in the oil samples with R/Ra, δD$_{CH4}$ or δ^{13}C$_{CO2}$ indicate the variations are largely caused by mantle-derived fluids, instead of biodegradation.

5.3. Variations of biomarkers with increasing intensity of mantle-derived fluids

Potentially, the mantle-derived fluids could affect biomarkers during or after hydrocarbon generation. Processes that occurred during hydrocarbon generation involved catalysis and hydrogenation in kerogen degradation (Jin et al., 2001, 2004), and increasing thermal maturity of source rocks (Peters and Moldowan, 1993; Requejo, 1994; Huang et al., 2016). In contrast, the mantle-derived fluids could alter biomarker distributions in petroleum by (1)

hydrogenolysis of the petroleum (e.g., Mango, 1992; Sun and Jin, 2000) and (2) thermal cracking (Zhao et al., 2005; Wang et al., 2006). In the Dongying Depression, Zhang et al. (2009) suggested that the mantle-derived fluids affect the chemical compositions in oil after hydrocarbon generation, based on (1) little similarity of the rare earth elements (REEs) between the oils and source rocks and (2) the correlation between REEs in the oil samples and R/Ra in their co-produced natural gas. This suggestion can be further evidenced by the fact that oil samples from the active zones are commonly accompanied by gases that have high R/Ra values indicative of mantle-derived helium that probably migrated and mixed with the oil/gas after it had been generated. Therefore, the mantle-derived fluids in the Dongying Depression probably occurred after oil generation and could affect the biomarkers in petroleum.

5.3.1. Variations of n-alkanes and isoprenoids

The abundance of *n*-C$_8$ to *n*-C$_{21}$ *n*-alkanes relative to the *n*-C$_{22}$ to *n*-C$_{45}$ *n*-alkanes (i.e., Σ*n*C$_{21-}$/Σ*n*C$_{22+}$) reflects the source of the organic matter (Peters et al., 2005). The Σ*n*C$_{21-}$/Σ*n*C$_{22+}$ values, in the study area, are not correlated with R/Ra and δ^{2}H$_{CH4}$, but are negatively correlated with δ^{13}C$_{CO2}$ (Fig. 5). The lack of correlation between Σ*n*C$_{21-}$/Σ*n*C$_{22+}$ and δ^{2}H$_{CH4}$ is consistent with the
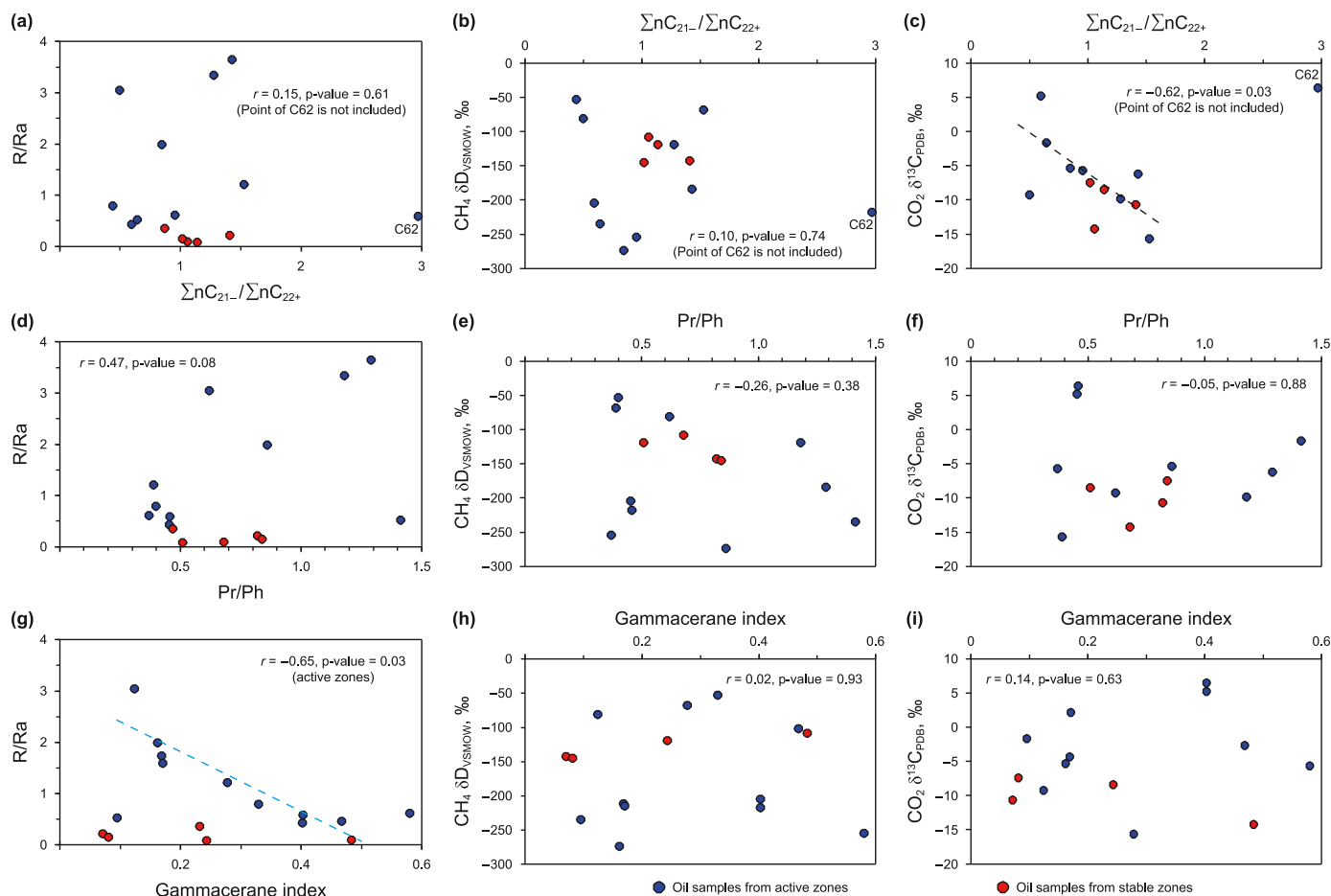
Fig. 5. Correlation diagrams of $\Sigma nC_{21-}/\Sigma nC_{22+}$ versus **(a)** R/Ra, **(b)** D_{CH4} and **(c)** $\delta^{13}C_{CO2}$, Pr/Ph versus **(d)** R/Ra, **(e)** D_{CH4} and **(f)** $\delta^{13}C_{CO2}$, and gammacerane index versus **(g)** R/Ra, **(h)** D_{CH4} and **(i)** $\delta^{13}C_{CO2}$.

Table 3
Selected biomarker parameters of crude oils in the Dongying Depression.

Magnitude of Mantle-derived fluid	Structure Location	Sampled Wells	Strata	Pr/Ph	Gammacerane index	C_{24} tetracyclic/C_{26} tricylic terpane	DBT/TF	DBF/TF
Active zones	Gaoqing- Pingnan Fault Belt	G42-hx1	Ek	n.d.	0.17	0.38	0.49	0.08
		G42-41	Ek	n.d.	0.17	0.38	0.32	0.28
		B166	O	1.18	n.d.	0.32	0.85	n.d.
		Bg24	O	1.29	n.d.	0.31	0.88	n.d.
		B4-6-41	Es$_4$	0.62	0.12	0.36	0.92	n.d.
		B338-13	Es$_3$	0.40	0.33	0.43	0.81	n.d.
	Shicun Fault Belt	B8	Es$_4$	0.37	0.58	0.57	0.14	0.33
		C13-404	Es$_3$+Es$_4$	0.45	0.40	0.48	0.25	0.30
		C62	Es$_3$	0.46	0.40	0.46	0.24	0.31
		Cg100-p1	O	n.d.	0.47	0.41	0.68	n.d.
		Cn93-4	O	0.39	0.28	0.39	1.00	n.d.
	Boxing Through	F143-5	Es$_4$	0.86	0.16	n.d.	0.18	0.22
		Z6-15	Es$_1$	1.41	0.10	0.32	0.31	0.23
Stable zones	Central Anticline Belt	S3-2-8	Es$_3$	0.82	0.07	0.33	0.90	n.d.
		H159	Es$_3$	0.68	0.48	0.39	0.90	n.d.
	Niuzhuang Trough	N25-35	Es$_3$	0.51	0.24	0.40	0.84	n.d.
		L61-x10	Es$_3$	0.84	0.08	0.34	0.78	n.d.
		C26-21	Es$_4$	0.47	0.23	0.40	0.82	n.d.

simulation experiment of Jin et al. (2007), which suggested that hydrogenation rarely affected the $\Sigma nC_{21-}/\Sigma nC_{22+}$ values. Their experiments also suggested that the thermal energy may lead to an increase in the $\Sigma nC_{21-}/\Sigma nC_{22+}$ ratio because the heat would cause cracking of the n-alkanes, especially the n-alkanes with heavy molecular weights (Jin et al., 2007). This suggestion, however, is inconsistent with the poor correlation between R/Ra and $\Sigma nC_{21-}/\Sigma nC_{22+}$ found in this study. Such a contradiction is probably related to the simulation experiments of Jin et al. (2007) that did not consider the effect of CO_2 on the n-alkanes. Indeed, studies on crude oils accompanying mantle-derived CO_2 in many other basins and experiments of CO_2 extraction evidenced that CO_2 preferred to
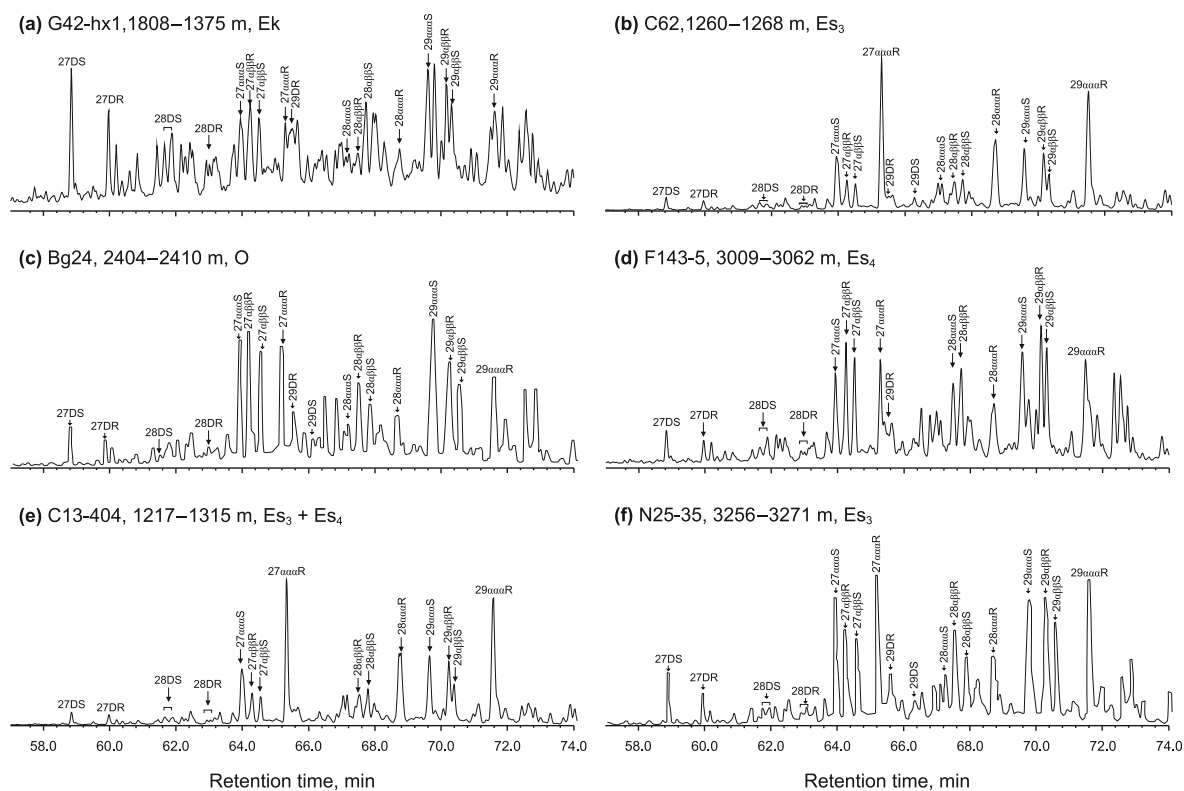
Fig. 6. Partial m/z 217 mass chromatograms of representative crude oils from the Dongying Depression. Peak assignments define stereochemistry at C-20 (S and R); $\alpha\alpha\alpha$ and $\alpha\beta\beta$ denote 5α(H), 14α(H), 17α(H)-steranes and 5α(H), 14β(H), 17β(H)-steranes, respectively; D = 13β(H), 17α(H)-diasteranes.

extract light n-alkanes with carbon numbers smaller than 20 (e.g., Li et al., 2006; Liu et al., 2017). In this study, the negative covariance between $\Sigma nC_{21-}/\Sigma nC_{22+}$ and $\delta^{13}C_{CO2}$ indicates that the mantle-derived CO_2 results in a decrease in the $\Sigma nC_{21-}/\Sigma nC_{22+}$ values, and thus, weakens the effect of thermal energy.

The Pr/Ph ratio is believed to be indicative of redox conditions
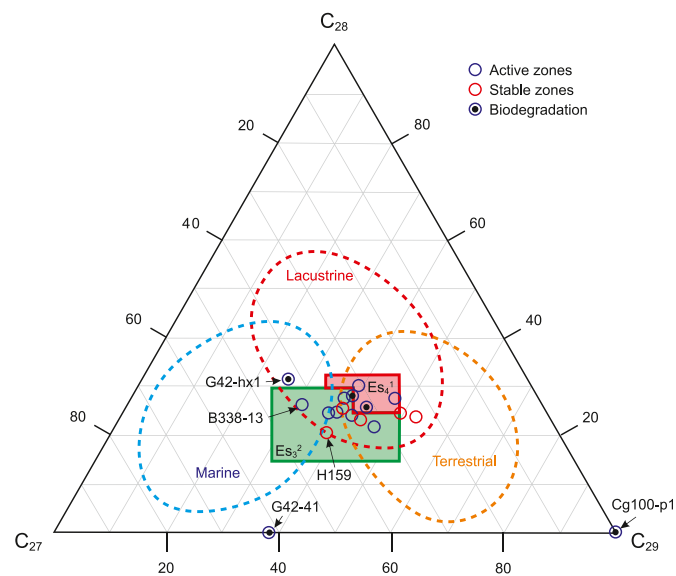
Fig. 7. Ternary diagram showing the relative distributions of C_{27}, C_{28} and C_{29} $\alpha\alpha\alpha$ (20R) steranes. Ranges of source rocks from Es_3^2 (green square) and Es_4^1 (red square) are modified from Tan et al. (2002). Ranges of terrestrial (yellow dashed lines), lacustrine (red dashed lines) and oceanic (blue dashed lines) environments are based on Peters and Moldowan (1993).

where the source rock was deposited (Powell and McKirdy, 1973). High Pr/Ph values (>3) typically indicate terrigenous organic matter deposited under oxic conditions (Powell and McKirdy, 1973). A ratio between 1 and 3 suggests oxic-suboxic conditions (Peters et al., 2005), whereas low Pr/Ph values (<1) suggest anoxic conditions (Didyk et al., 1978; Peters et al., 2005; Cheng et al., 2013). Such suggestions, however, are not applicable due to the influences of mantle-derived fluids. Simulation experiments, for example, evidenced that Pr/Ph increased as temperature increased (Jin et al., 2007) or the intensity of hydrogenation dropped (Jin et al., 2004). In this study, the Pr/Ph values are poorly correlated with R/Ra, δ^2H_{CH4}, and $\delta^{13}C_{CO2}$ (Fig. 5(d)–(f)). The lack of any evidence for an increase in the Pr/Ph ratio may suggest that the thermal and hydrogenation effects may balance out.

5.3.2. Variations of steranes and terpanes

The C_{27} sterane is probably derived from marine organic matter, whereas C_{28} and C_{29} steranes reflect the contributions from lacustrine algae and terrestrial plants, respectively (Huang and Meinschein, 1979; Peters et al., 2005; Samuel et al., 2009). In the Dongying Depression, the relative abundances of C_{27}, C_{28} and C_{29} $\alpha\alpha\alpha$ (20R) steranes change little with increasing heat, H_2 and CO_2 from the mantle-derived fluids (Supplementary Fig. S1). Moreover, their relative abundances show little difference between the active and stable zones (Fig. 7). Considering that C_{27}, C_{28} and C_{29} $\alpha\alpha\alpha$ (20R) steranes can be cracked by thermal stress (Peters and Moldowan, 1993; Requejo, 1994), the stable values of their relative abundances indicate these regular steranes may have been subjected to similar levels of alteration caused by mantle-derived fluids. As such, there is no significant variation in the relative abundances of C_{27}, C_{28} and C_{29} $\alpha\alpha\alpha$ (20R) steranes in the oils that have been affected by mantle-derived fluids.

Gammacerane, which is a non-hopanoid C_{30} triterpane,
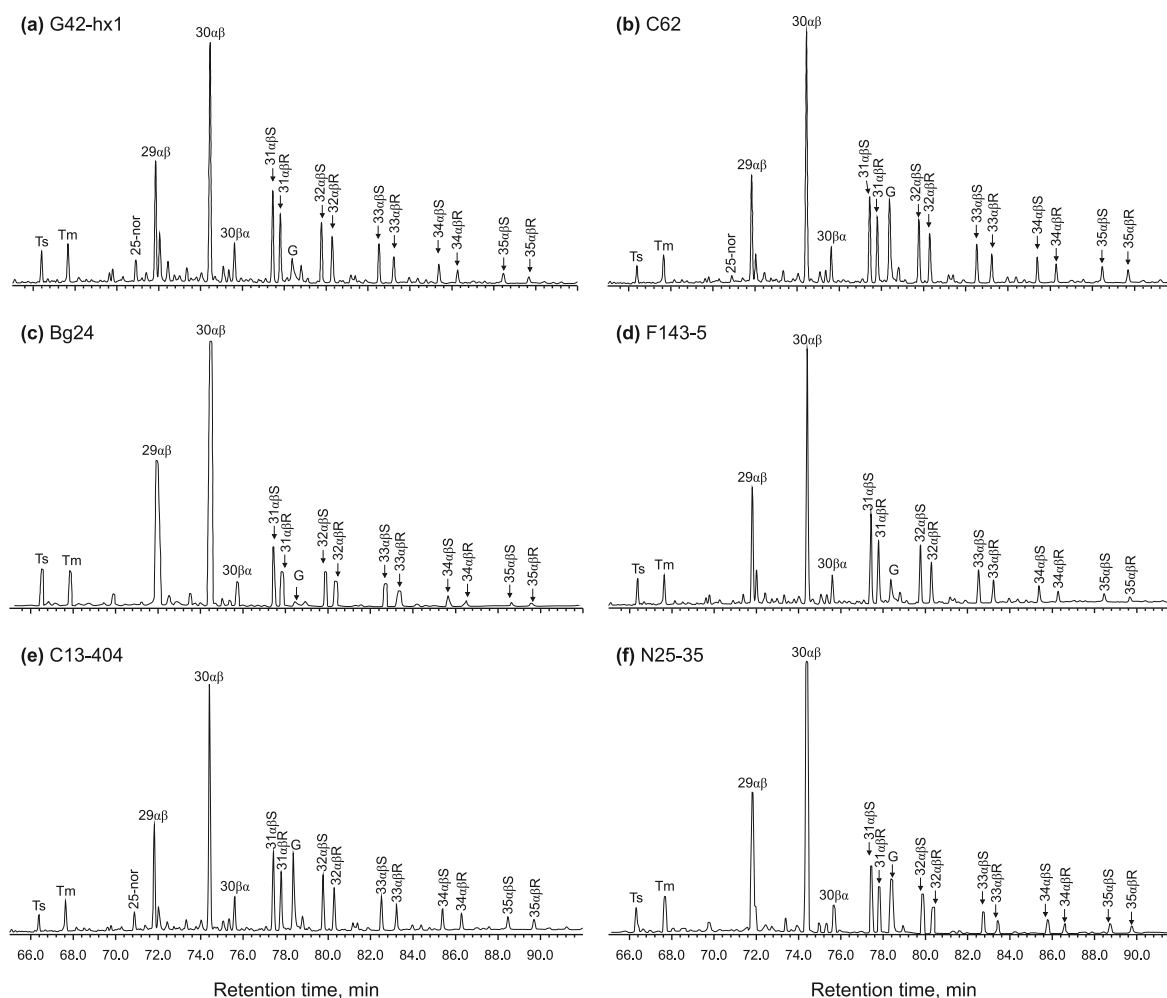
Fig. 8. Partial m/z 191 mass chromatograms of representative crude oils from the Dongying Depression. Peak assignments define stereochemistry at C-22 (S and R); αβ and βα denote 17α(H)-hopanes and 17β(H)-moretanes, respectively; Ts = C_{27}18α(H), 22, 29, 30-trisnorneohopane; Tm=C_{27}17α(H), 22, 29, 30-trisnorhopane; 25-nor = C_{29} 25-norhopane; G: gammacerane.

originates from phototrophic bacterial, which prefers hypersaline environments (Peters and Moldowan, 1993). The high gammacerane index (>0.2) indicates the water column during sedimentation was stratified due to salinity (Venkatesan, 1989; Sinninghe Damsté et al., 1995; Marynowski et al., 2000). As such, the variable values of gammacerane index in the oil samples from the stable zones point to different source rocks. In the oil samples from the active zones, in contrast, a negative covariance is apparent between the gamma-cerane index and R/Ra (Fig. 5(g)–(i)), suggesting the gammacerane index may not be applicable for tracing the source rock in the zones affected by mantle-derived fluids. This suggestion is consistent with the thermal simulation experiments conducted by Liu (2008). His experiments suggested that the gammacerane index increased as temperatures was raised to 350 °C, but then decreased as the temperature continued to increase. As such, in the active zones, the negative covariance between the gammacerane index and the R/Ra values indicates a reaction temperature of greater than 350 °C.

The C_{31}/C_{30} hopane is commonly used as an indicator of the depositional environments of source rocks (Peters et al., 2005). The oil from marine environments, for example, is characterized by C_{31}/C_{30} hopane greater than 0.25 (Peters et al., 2005). Accordingly, the C_{31}/C_{30} hopane ratio in this study, which is greater than 0.3, points to deposition in a marine environment. This, however, is not true, given that (1) marine environments rarely occurred in the

Dongying Depression during the Cenozoic, and (2) the main source rocks in the Dongying Depression probably developed from sediments that were deposited in a lacustrine environment (Hu et al., 1989; Group of Shengli Oil Field Compiling Petroleum Geology, 1993). The erroneous explanation derived by using C_{31}/C_{30} hopane may be attributed to the effect of mantle-derived fluids on the C_{31}/C_{30} hopane. The negative correlation between the C_{31}/C_{30} hopane and δ^2H_{CH4}, and the positive correlation between the C_{31}/C_{30} hopane and $\delta^{13}C_{CO2}$ (Fig. 9(b) and (c)) suggest this parameter can be altered by H_2 and CO_2. In contrast, the lack of correlation between C_{31}/C_{30} hopane and R/Ra (Fig. 9(a)) suggests that the thermal energy has little impact on the C_{31}/C_{30} hopane. Such relationships, however, seem incompatible with the suggestion that the C–C bonds in high molecular weight hopane (i.e., C_{31}) are more likely to be fractured by thermal energy than those that have a low molecular weight (Zhu et al., 2008). Such a contradiction may arise because previous studies have not considered the effects of H_2 and CO_2 released from mantle-derived fluids. Therefore, mantle volatiles may have a greater impact on the C_{31}/C_{30} hopane than the thermal input. There is, however, no evidence to indicate the relative importance of hydrogenation and CO_2 on C_{31}/C_{30} hopane.

The abundance of C_{24} tetracyclic is typically considered indicative of a hypo-saline environment, whereas the C_{26} tricyclic terpane is used as an indicator of the contribution from land plants
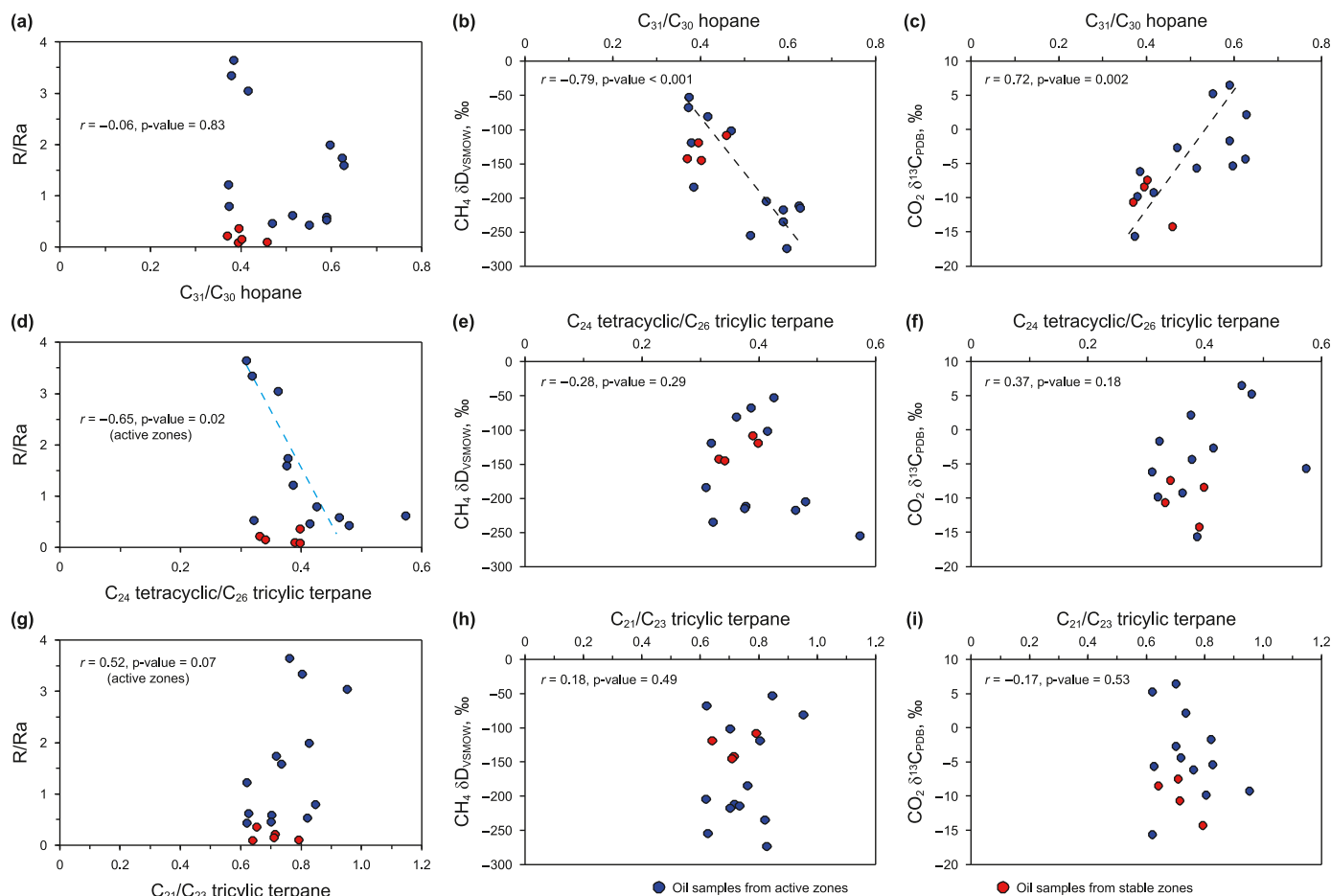
Fig. 9. Correlation diagrams of C_{31}/C_{30} hopane versus **(a)** R/Ra, **(b)** D_{CH4} and **(c)** $\delta^{13}C_{CO2}$, C_{24} tetracyclic/C_{26} tricylic terpane versus **(d)** R/Ra, **(e)** D_{CH4} and **(f)** $\delta^{13}C_{CO2}$, and C_{21}/C_{23} tricylic terpane versus **(g)** R/Ra, **(h)** D_{CH4} and **(i)** $\delta^{13}C_{CO2}$.

(Azevedo et al., 1992; Peters and Moldowan, 1993). As such, the ratio of C_{24} tetracyclic/C_{26} tricyclic terpane is commonly examined during oil-source correlation. In this study, C_{24} tetracyclic/C_{26} tricylic terpane and R/Ra exhibit a negative covariance (Fig. 9(d)), indicating that abnormal heat energy could lead to a decrease in this parameter. Such a correlation is compatible with the suggestion that tricyclic terpanes are thermally more stable than other terpanes (Peters and Moldowan, 1993). The δ^2H_{CH4} and $\delta^{13}C_{CO2}$ values, in contrast, are poorly correlated with the C_{24} tetracyclic/C_{26} tricyclic terpane (Fig. 9(e) and (f)), suggesting that H_2 and CO_2 have little influence on this parameter.

Given that tricyclic terpanes are resistant to biodegradation and maturity (Seifert and Moldowan, 1979; Peters and Moldowan, 1993), the distributions of tricyclic terpanes are widely used for oil-source correlations (Bao et al., 2012). In this study, the variation of C_{21}/C_{23} tricyclic terpane indicates that the oils in the stable zones seem relatively more dominated by C_{23} component than the oils in the active zones (Fig. 9(g)). Such phenomenon is consistent with the suggestion that abnormal heat may break the C−C bounds in the high molecular components and lead to a relatively increase in the low molecular weight components (Zhu et al., 2008). The C_{21}/C_{23} tricyclic terpane, in contrast, is not correlated with δ^2H_{CH4} or $\delta^{13}C_{CO2}$ values (Fig. 9(h) and (i)), indicating that H_2 and CO_2 are probably not the key factors that affect the variation of C_{21}/C_{23} tricyclic terpane.

5.3.3. Variations of DBT/TF and DBF/TF

The distribution patterns of TF are believed to reflect the type of source rock and their depositional environments (Hughes, 1984). The relative abundance of DBT (i.e., DBT/TF), for example, can be indicative of a suboxic environment, whereas that of DBF (i.e., DBF/TF) has been used to indicate an oxic environment (Fan et al., 1990; Radke et al., 2000; Chang et al., 2011). Previous studies attributed the systematic changes of polycyclic aromatic hydrocarbons (PAHs) to thermal energy, as free radicals derived from cracking oils could form PAHs by pyro-synthesis (Yunker et al., 2002; Zhu et al., 2008). In this study, however, the DBT/TF or DBF/TF ratios change little with increasing R/Ra. Instead, DBT/TF seems to be correlated with δ^2H_{CH4} and $\delta^{13}C_{CO2}$, indicating hydrogenation would cause an increase of DBT/TF (Supplementary Fig. S2(b)), and CO_2 would lead to a decrease in DBT/TF (Supplementary Fig. S2(c)). Therefore, H_2 and CO_2 released from mantle-derived fluids may play a more important role on the distributions of TF than thermal energy. This is probably because hydrogen gas could lead to a reducing environment, which favors the pyro-synthetic processes of DBT, whereas CO_2 could result in an oxidizing environment favoring the pyro-synthetic processes of DBF. There is, however, little evidence to evaluate the relative importance of H_2 and CO_2 on the variations of DBT/TF and DBF/TF.

5.4. Implications for oil-source correlation

Source rocks from Es_4^1 are characterized by (1) pristane/phytane

(i.e., Pr/Ph) < 1, (2) C_{27}, C_{28} and C_{29} $\alpha\alpha\alpha$ 20R steranes having relatively equal distribution with a slight predominance of C_{29} steranes, (3) high concentrations of gammacerane, with the gammacerane index (i.e., gammacerane/$\alpha\beta C_{30}$ hopane) averaging 1.1, and (4) C_{24} tetracyclic/C_{26} tricyclic terpane values that are typically lower than 0.8 (Tan et al., 2002; Zhu et al., 2004b; Li et al., 2007). The biomarkers in the source rock from Es_3^2, in contrast, are characterized by the followings: (1) Pr/Ph is greater than 1, typically varying from 1.0 to 2.5, (2) the distribution of C_{27} $\alpha\alpha\alpha$ 20R steranes relative to C_{29} is highly variable, with C_{27}/C_{29} and C_{28}/C_{29} varying from 0.67 to 2.73 and from 0.55 to 1.02, respectively (3) the gammacerane concentration is low, with the gammacerane index less than 0.1, and (4) C_{24} tetracyclic/C_{26} tricyclic terpane values are typically greater than 1 (Tan et al., 2002; Zhu et al., 2004b; Li et al., 2007).

Based on biomarkers, the oil-source correlation has been comprehensively investigated throughout the Dongying Depression (e.g., Tan et al., 2002; Zhu et al., 2004b; Zhang et al., 2004; Li et al., 2007). Many of the results, however, are controversial. Previous studies, for example, suggested that the oil from the Niuzhuang Oilfield was derived largely from Es_3^2 source rocks (Zhu et al., 2004a, 2004b), whereas Li et al. (2007) stressed a greater contribution from Es_4^1 source rock. Tan et al. (2002) suggested that oil in the Gaoqing and Boxing oilfields was from Es_4^1 source rocks and oil from the Liangjialou Oilfield was from Es_3^2 (Tan et al., 2002). Such oil-source correlations, however, were challenged by Zhu et al. (2004b), who suggested that those oils were the mixtures of oils from Es_3^2 and Es_4^1 source rocks. The root cause for this controversy is probably the injudicious use of biomarkers that have been altered by mantle-derived fluids, since oils can lose their original signatures due to high thermal stress (e.g., Simoneit et al., 1996,; Zhang et al., 2009; Huang et al., 2016), hydrogenation (e.g., Jin et al., 2007), and CO_2. As such, the influence of mantle-derived fluid has to be considered before oil-source correlations.

Based on its low R/Ra (<0.1), the oil (i.e., N25-35) from the Niuzhuang Oilfield seems to have experienced little alteration by mantle-derived fluids. This, together with its low level of biodegradation, means its original signature may have been retained. As such, this oil reflects a great contribution from Es_4^1 source rock, based on its biomarker distributions, including Pr/Ph (0.51), C_{27}/C_{29} $\alpha\alpha\alpha$ 20R steranes (0.78), C_{28}/C_{29} $\alpha\alpha\alpha$ 20R steranes (0.53), gammercerane index (0.24), and C_{24} tetracyclic/C_{26} tricyclic terpane (0.40).

Given that the relative abundances of C_{27}, C_{28} and C_{29} $\alpha\alpha\alpha$ (20R) steranes may not have been altered by mantle-derived fluids, they can be used for oil-source correlations in the oils that have suffered minimal levels of biodegradation (Fig. 7). In comparison to the source rocks from Es_3^2 and Es_4^1 (Tan et al., 2002), oil samples, except for B338−13 and H159, are located close to the boundary between these two source rocks (Fig. 7), indicating that most formed by mixing of oils sourced from Es_3^2 and Es_4^1. In contrast, oils from B338−13 and H159 show similar distribution patterns of C_{27}, C_{28} and C_{29} $\alpha\alpha\alpha$ (20R) steranes with Es_3^2, indicating they are mainly sourced from Es_3^2. Such oil-source correlations, however, cannot be identified by using Pr/Ph, gammacerane index and C_{24} tetracyclic/C_{26} tricyclic terpane, which are routinely used to discriminate between Es_4^1-sourced oils and Es_3^2-sourced oils (Huang and Pearson, 1999; Li et al., 2003, 2007; Pang et al., 2003; Tan et al., 2002). The correlation between Pr/Ph and gammacerane index, for example, would lead to an erroneous conclusion, which suggests that the oils were largely derived from the Es_4^1 source rocks (Fig. 10). Similarly, the C_{24} tetracyclic/C_{26} tricyclic terpane ratios are mostly lower than 1 (Table 3), falling within the range of Es_4^1 source rock. Therefore, biomarkers in the active zones have to be corrected before any oil-source correlation can be derived from them. Nevertheless, the manner of correcting those biomarkers remains open to debate.
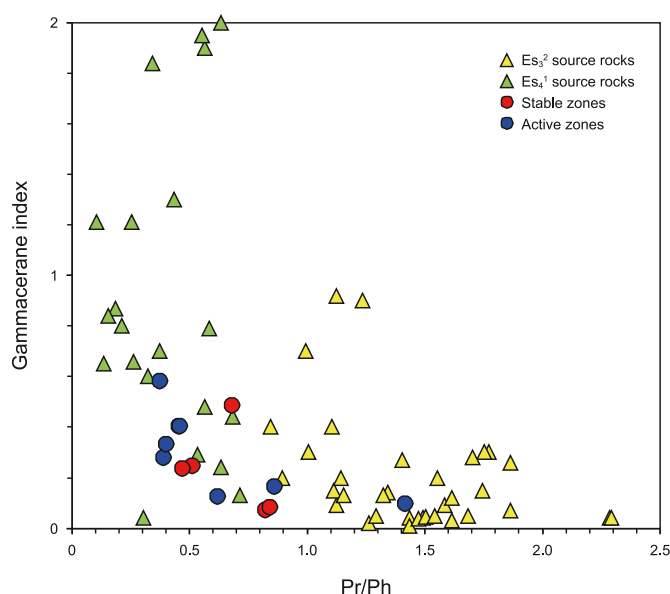

Fig. 10. Variation of Pr/Ph with gammacerane index in oils (blue and red circles) and source rocks (yellow and green triangles) in the Dongying Depression. The source rock data are based on the results from Zhu and Jin (2003).

6. Conclusions

The flux intensity and chemical compositions of mantle-derived fluids in the Dongying Depression are variable from locality to locality. The zones close to the deep faults show more intense activities of mantle-derived fluids than in the stable zones, which are relatively distant from deep faults. The mantle-derived fluids on the north part of the Dongying Depression have more H_2 and less CO_2 than those on the south part.

The correlations between R/Ra and variable biomarkers, which are routinely used to make oil-source correlations, indicate that thermal energy can lead to alteration of the Pr/Ph, the gammacerane index, as well as the C_{24} tetracyclic/C_{26} tricylic terpane and C_{21}/C_{23} tricylic terpane. The plots of biomarkers versus to $\delta^2 H_{CH4}$ and $\delta^{13}C_{CO2}$ reveal thermal cracking of C−C bonds in high molecular weight components and pyro-synthesis of PAHs could be impeded by the H_2 and/or CO_2 from mantle-derived fluids. Hydrogen gas, for example, could result in systematic changes of Pr/Ph, C_{31}/C_{30} hopane, and DBT/TF, whereas CO_2 could affect the values of $\Sigma nC_{21-}/\Sigma nC_{22+}$, C_{31}/C_{30} hopane and DBT/TF. The mantle-derived fluids, in contrast, result in no significant variations in the relative distributions of C_{27}, C_{28} and C_{29} $\alpha\alpha\alpha$ (20R) steranes. Based on relative abundances of C_{27}, C_{28} and C_{29} $\alpha\alpha\alpha$ (20R) steranes, the oil samples collected from the Dongying Depression are mostly the mixtures of Es_4^1 and Es_3^2 rock systems.

CRediT authorship contribution statement

Ting Liang: Writing − review & editing, Writing − original draft, Supervision, Project administration, Methodology, Investigation, Funding acquisition, Formal analysis. **Mei-Lin Jiao:** Visualization, Formal analysis. **Xin-Liang Ma:** Formal analysis, Data curation. **Liu-Ping Zhang:** Supervision, Resources.

Declaration of competing interest

The authors declare that they have no known competing financial interests or personal relationships that could have

appeared to influence the work reported in this paper.

Acknowledgments

Appendix A. Supplementary data

Supplementary data to this article can be found online at https://doi.org/10.1016/j.petsci.2024.06.002.

References

Allen, M.B., Macdonald, D.I.M., Zhao, X., et al., 1997. Early Cenozoic two-phase extension and late Cenozoic thermal subsidence and inversion of the Bohai Basin, northern China. Mar. Pet. Geol. 14 (7–8), 951–972. https://doi.org/10.1016/S0264-8172(97)00027-5.

Azevedo, D.A., Aquino Neto, F.R., Simoneit, B.R.T., et al., 1992. Novel series of tricyclic aromatic terpanes characterized in Tasmanian tasmanite. Org. Geochem. 18 (1), 9–16. https://doi.org/10.1016/0146-6380(92)90138-N.

Bao, J.P., Kong, J., Zhu, C.S., et al., 2012. Geochemical characteristics of a novel kind of marine oils from Tarim Basin. Acta Sedimentol. Sin. 30 (3), 580–587. https://doi.org/10.14027/j.cnki.cjxb.2012.03.009 (in Chinese).

Bigi, S., Beaubien, S.E., Ciotoli, G., et al., 2014. Mantle-derived CO_2 migration along active faults within an extensional basin margin (Fiumicino, Rome, Italy). Tectonophysics 637, 137–149. https://doi.org/10.1016/j.tecto.2014.10.001.

Botz, R., Wehner, H., Schmitt, M., et al., 2002. Thermogenic hydrocarbons from the offshore Calypso hydrothermal field, Bay of Plenty, New Zealand. Chem. Geol. 186 (3–4), 235–248. https://doi.org/10.1016/S0009-2541(01)00418-1.

Caracausi, A., Martelli, M., Nuccio, P.M., et al., 2013. Active degassing of mantle-derived fluid: a geochemical study along the Vulture line, southern Apennines (Italy). J. Volcanol. Geotherm. Res. 253, 65–74. https://doi.org/10.1016/j.jvolgeores.2012.12.005.

Caracausi, A., Nuccio, P.M., Favara, R., et al., 2008. Gas hazard assessment at the Monticchio crater lakes of Mt. Vulture, a volcano in southern Italy. Terra. Nova 21 (2), 83–87. https://doi.org/10.1111/j.1365-3121.2008.00858.x.

Chang, X.C., Han, Z.Z., Shang, X.F., et al., 2011. Geochemical characteristics of aromatic hydrocarbons in crude oils from the Linnan Subsag, Shandong Province, China. Chin. J. Geochem. 30, 132–137. https://doi.org/10.1007/s11631-011-0494-6.

Cheng, P., Xiao, X.M., Tian, H., et al., 2013. Source controls on geochemical characteristics of crude oils from the Qionghai Uplift in the western Pearl river Mouth basin, offshore south China Sea. Mar. Pet. Geol. 40, 85–98. https://doi.org/10.1016/j.marpetgeo.2012.10.003.

Clifton, C.G., Walters, C.C., Simoneit, B.R.T., 1990. Hydrothermal petroleum from Yellowstone National Park, Wyoming, U.S.A. Appl. Geochem. 5 (1–2), 169–191. https://doi.org/10.1016/0883-2927(90)90047-9.

Dai, J., Hu, G., Ni, Y., et al., 2009. Natural gas accumulation in Eastern China. Energy Explor. Exploit. 27 (4), 225–259. https://doi.org/10.1260/014459809789996147.

Didyk, B., Simoneit, B.R.T., Brassell, S.C., et al., 1978. Organic geochemical indicators of palaeoenvironmental conditions of sedimentation. Nature 272, 216–222. https://doi.org/10.1038/272216a0.

Fan, P., Philp, R.P., Li, Z.X., et al., 1990. Geochemical characteristics of aromatic hydrocarbons of crude oils and source rocks from different sedimentary environments. Org. Geochem. 16 (1–3), 427–435. https://doi.org/10.1016/0146-6380(90)90059-9.

Fisher, R.A., 1992. Statistical Methods for Research Workers. Breakthroughs in Statistics. Springer, New York.

Group of Shengli Oil Field Compiling Petroleum Geology, 1993. Shengli Oilfields. Petroleum Geology of China 6.

Guan, L.F., Liu, W., Cao, C.H., et al., 2023. Origin, spatial distribution, and geological implications of helium in fluids from the Tan-Lu fault zone. Geochim 52 (5), 570–581. https://doi.org/10.19700/j.0379-1726.2023.05.003 (in Chinese).

Hao, X.F., 2007. Conduit systems and reservoir-controlled model searching. In: Dongying Depression. Zhejiang University, China, p. 105.

Hu, A.P., Dai, J.X., Yang, C., et al., 2009. Geochemical characteristics and distribution of CO2 gas fields in Bohai Bay Basin. Pet. Explor. Dev. 36 (2), 181–189. https://doi.org/10.1016/S1876-3804(09)60118-X.

Hu, J., Xu, S., Tong, X., Wu, H., 1989. The Bohai Bay Basin. In: Zhu, X. (Ed.), Chinese Sedimentary Basins. Elsevier, Amsterdam, pp. 89–105.

Huang, W.Y., Meinschein, W.G., 1979. Sterols as ecological indicators. Geochemica et Cosmochemica Acta 43 (5), 739–745. https://doi.org/10.1016/0016-7037(79)90257-6.

Huang, H.P., Pearson, M.J., 1999. Source rock palaeoenvironments and controls on the distribution of dibenzothiophenes in lacustrine crude oils, Bohai Bay Basin, eastern China. Org. Geochem. 30 (11), 1455–1470. https://doi.org/10.1016/S0146-6380(99)00126-6.

Huang, H.P., Zhang, S.C., Su, J., 2016. Palaeozoic oil-source correlation in the Tarim Basin, NW China: A review. Org. Geochem. 94, 32–46. https://doi.org/10.1016/j.orggeochem.2016.01.008.

Hughes, W.B., 1984. Use of thiophenic organosulfer compounds in characterizing crude oils derived from carbonate versus siliciclastic sources. In: Palacas, J.G. (Ed.), AAPG Studies in Geology Volume 18: Petroleum Geochemistry and Source Rock Potential of Carbonate Rocks. AAPG, Tulsa, USA, pp. 181–196.

Jiang, Y.L., Rong, Q.H., Song, J.Y., 2003. Formation and distribution of oil and gas pools in boxing area of the Dongying depression, the Bohai Bay Basin. Petroleum Geology and Experiment 25 (5), 452–457. https://doi.org/10.11781/sysydz200305452 (in Chinese).

Jin, Z., Hu, W., Zhang, L., et al., 2007. The Activities of Deep Fluids and Their Effects on Generation of Hydrocarbon. China Science Publishing and Media Ltd, Beijing (in Chinese).

Jin, Z.J., Sun, Y.Z., Yang, L., 2001. Influences of deep fluids on organic matter of source rocks from the Dongying Depression, East China. Energy Explor. Exploit. 19 (5), 479–486. https://doi.org/10.1260/0144598011492606.

Jin, Z.J., Zhang, L.P., Yang, L., et al., 2004. A preliminary study of mantle-derived fluids and their effects on oil/gas generation in sedimentary basins. J. Petrol. Sci. Eng. 41 (1–3), 45–55. https://doi.org/10.1016/S0920-4105(03)00142-6.

Jin, Z.J., Zhang, L.P., Zeng, J.H., et al., 2002. Multi-origin alkanes related to CO2-rich, mantle-derived fluid in Dongying Sag, Bohai Bay Basin. Chin. Sci. Bull. 47 (20), 1756–1760. https://doi.org/10.1007/BF03183323.

King, C.Y., 1986. Gas geochemistry applied to earthquake prediction: an overview. J. Geophys. Res. 91 (B12), 12269–12281. https://doi.org/10.1029/JB091iB12p12269.

Li, M.T., Shan, W.W., Liu, X.G., et al., 2006. Laboratory study on miscible oil displacement mechanism of supercritical carbon dioxide. Acta Petrol. Sin. 27 (3), 80–83. https://doi.org/10.3321/j.issn:0253-2697.2006.03.017 (in Chinese).

Li, Q., You, X.L., Jiang, Z.X., et al., 2024. Lacustrine deposition in response to the middle eocene climate evolution and tectonic activities, Bohai Bay Basin, China. Mar. Pet. Geol. 163, 106811. https://doi.org/10.1016/j.marpetgeo.2024.106811.

Li, S.M., Pang, X.Q., Li, M.W., et al., 2003. Geochemistry of petroleum systems in the Niuzhuang south slope of Bohai Bay Basin-part 1: Source rock characterization. Org. Geochem. 34 (3), 389–412. https://doi.org/10.1016/S0146-6380(02)00210-3.

Li, S.M., Qiu, G.Q., Jiang, Z.X., et al., 2007. Origin of the subtle oils in the Niuzhuang Sag. Earth Science 32 (2), 213–218 (in Chinese). CNKI:SUN:DQKX.0.2007-02-008.

Liu, G., 2008. Thermal simulation study of crude oil from well S74 in the Tarim Basin (I) — geochemical characteristics of the simulation products. Petroleum Geology and Experiment 30 (2), 179–185 (in Chinese).

Liu, Q.Y., Wu, X.Q., Zhu, D.Y., et al., 2021. Generation and resource potential of abiogenic alkane gas under organic-inorganic interactions in petroliferous basins. Journal of Natural Gas Geoscience 6 (2), 79–87. https://doi.org/10.1016/j.jnggs.2021.04.003.

Liu, Q.Y., Zhu, D.Y., Jin, Z.J., et al., 2017. Effects of deep CO2 on petroleum and thermal alteration: The case of the Huangqiao oil and gas field. Chem. Geol. 469, 214–229. https://doi.org/10.1016/j.chemgeo.2017.06.031.

Liu, X., Xu, S., Li, P., 1995. Non-hydrocarbon (CO2 and He) origin and accumulation, exploration and development technology, and synthesis use. National Eighth-Five-Plan Science and Technology Project. No. 85-925a-08, Beijing (in Chinese).

Lyon, G.L., Hulston, J.R., 1984. Carbon and hydrogen isotopic compositions of New Zealand geothermal gases. Geochim. Cosmochim. Acta 48 (6), 1161–1171. https://doi.org/10.1016/0016-7037(84)90052-8.

Mango, F.D., 1992. Transition metal catalysis in the generation of petroleum and natural gas. Geochim. Cosmochim. Acta 56 (1), 553–555. https://doi.org/10.1016/0016-7037(92)90153-A.

Marynowski, L., Narkiewicz, M., Grelowski, C., 2000. Biomarkers as environmental indicators in a carbonate complex, example from the Middle to Upper Devonian, Holy Cross Mountains, Poland. Sediment. Geol. 137 (3–4), 187–212. https://doi.org/10.1016/S0037-0738(00)00157-3.

Niu, Z.C., Wang, Y.S., Wang, X.J., et al., 2022. Characteristics of crude oil with different sulfur content and genesis analysis of high-sulfur crude oil in eastern section of southern slope of Dongying Sag. Petroleum Geology and Recovery Efficiency 29 (5), 15–27. https://doi.org/10.13673/j.cnki.cn37-1359/te.202108024 (in Chinese).

Nuccio, P.M., Caracausi, A., Costa, M., 2014. Mantle-derived fluids discharged at the Bradanic foredeep/Apulian foreland boundary: The Maschito geothermal gas emissions (southern Italy). Mar. Pet. Geol. 55, 309–314. https://doi.org/10.1016/j.marpetgeo.2014.02.009.

Palcsu, L., Vetö, I., Futó, I., et al., 2014. In-reservoir mixing of mantle-derived CO2 and metasedimentary CH4-N2 fluids — Nobel gas and stable isotope study of two multistacked fields (Pannonian Basin System, W-Hungary). Mar. Pet. Geol. 54, 216–227. https://doi.org/10.1016/j.marpetgeo.2014.03.013.

Pang, X.Q., Li, M.W., Li, S.M., et al., 2003. Geochemistry of petroleum systems in the Niuzhuang south slope of Bohai Bay Basin-part 2: Evidence for significant

contribution of mature source rocks to "immature oils" in the Bamianhe field. Org. Geochem. 34 (4), 931—950. https://doi.org/10.1016/j.orggeochem.2004.12.001.

Peters, K.E., Moldowan, J.M., 1993. The biomarker guide. Interpreting Molecular Fossils in Petroleum and Ancient Sediments. Prentice Hall, New Jersey.

Peters, K.E., Walters, C.C., Moldowan, J.M., 2005. The Biomarker Guide. In: Biomarkers and Isotopes in Petroleum Exploration and Earth History, vol. 2. Cambridge University Press, Cambridge.

Powell, T.G., McKirdy, D.M., 1973. Relationship between ratio of pristane to phytane in crude oil composition and geological environment in Australia. Nat. Phys. Sci. (Lond.) 243, 37—39. https://doi.org/10.1038/physci243037a0.

Radke, M., Vriend, S.P., Ramanampisoa, L.R., 2000. Alkyldibenzofurans in terrestrial rocks: influence of organic facies and maturation. Geochim. Cosmochim. Acta 64 (2), 275—286. https://doi.org/10.1016/S0016-7037(99)00287-2.

Requejo, A.G., 1994. Maturation of petroleum source rocks. II. Quantitative changes in extractable hydrocarbon content and composition associated with hydrocarbon generation. Org. Geochem. 21 (1), 91—105. https://doi.org/10.1016/0146-6380(94)90089-2.

Samuel, O.J., Cornford, C., Jones, M., et al., 2009. Improved understanding of the petroleum systems of the Niger Delta Basin, Nigeria. Org. Geochem. 40 (4), 461—483. https://doi.org/10.1016/j.orggeochem.2009.01.009.

Schoell, M., 1980. The hydrogen and carbon isotopic composition of methane from natural gases of various origins. Geochim. Cosmochim. Acta 44 (5), 649—661. https://doi.org/10.1016/0016-7037(80)90155-6.

Seifert, W.K., Moldowan, J.M., 1979. The effect of biodegradation on steranes and terpanes in crude oils. Geochimica et Coschimica Acta 43 (1), 111—126. https://doi.org/10.1016/0016-7037(79)90051-6.

Shen, B.J., Huang, Z.L., Liu, H.W., et al., 2007. Geochemistry and origin of gas pools in the Gaoqing-Pingnan fault zone, Jiyang Depression. Chin. J. Geochem. 26 (4), 446—454. https://doi.org/10.1007/s11631-007-0446-3.

Simoneit, B.R.T., Leif, R.N., Ishiwatari, R., 1996. Phenols in hydrothermal petroleums and sediment bitumen from Guaymas Basin, Gulf of California. Org. Geochem. 24 (3), 377—388. https://doi.org/10.1016/0146-6380(96)00008-3.

Sinninghe Damsté, J.S., Kenig, F., Koopmans, M.P., et al., 1995. Evidence for gammacerane as an indicator of water column stratification. Geochim. Cosmochim. Acta 59 (9), 1895—1900. https://doi.org/10.1016/0016-7037(95)00073-9.

Sun, Y.Z., Jin, Y.J., 2000. Influences of basin brines on hydrocarbons of the Anthracosia shales from southwest Poland. ACTA GEOL SIN 74 (1), 93—101. https://doi.org/10.1111/j.1755-6724.2000.tb00435.x.

Tan, L.J., Jiang, Y.L., Su, C.Y., et al., 2002. The characters of source rock and oil source in the Boxing Oilfield, Dongying depression. J. Univ. Pet., China (Ed. Nat. Sci.) 26 (5), 1—5 (in Chinese). CNKI:SUN:SYDX.0.2002-05-001.

Venkatesan, M.I., 1989. Tetrahymanol: its widespread occurrence and geochemical significance. Geochim. Cosmochim. Acta 53 (11), 3095—3101. https://doi.org/10.1016/0016-7037(89)90190-7.

Wang, X.F., Liu, Q.Y., Liu, W.H., et al., 2022. Accumulation mechanism of mantle-derived helium resources in petroliferous basins, eastern China. SCI CHINA EARTH SCI 65 (12), 2322—2334. https://doi.org/10.1007/s11430-022-9977-8.

Wang, Y.P., Zhang, S.C., Wang, F.Y., et al., 2006. Thermal cracking history by laboratory kinetic simulation of Palaeozoic oil in eastern Tarim Basin, NW China, implications for the occurrence of residual oil reservoirs. Org. Geochem. 37 (12), 1803—1815. https://doi.org/10.1016/j.orggeochem.2006.07.010.

Whiticar, M.J., 1990. A geochemical perspective of natural gas and atmospheric methane. Org. Geochem. 16 (1—3), 531—547. https://doi.org/10.1016/0146-6380(90)90068-B.

Xu, H.Y., Hou, D.J., Löhr, S.C., et al., 2023. Millimetre-scale biomarker heterogeneity in lacustrine shale identifies the nature of signal-averaging and demonstrates anaerobic respiration control on organic matter preservation and dolomitization. Geochim. Cosmochim. Acta 348, 107—121. https://doi.org/10.1016/j.gca.2023.03.008.

Xu, Y.C., 1996. Mantle-derived rare gas in natural gas. Earth Sci. Front. 3 (3), 63—71 (in Chinese). CNKI:SUN:DXQY.0.1996-03-006.

Yang, Z.C., Zhang, J.L., 2008. Biomarkers of crude oils and oil-source correlation in the south slope of the Dongying depression. Periodical of Ocean University of China 38 (3), 453—460. https://doi.org/10.3969/j.issn.1672-5174.2008.03.012 (in Chinese).

Yunker, M.B., Macdonald, R.W., Vingarzan, R., et al., 2002. PAHs in the Fraser River basin: a critical appraisal of PAH ratios as indicators of PAH source and composition. Org. Geochem. 33 (4), 489—515. https://doi.org/10.1016/S0146-6380(02)00002-5.

Zhang, K.J., 1997. North and South China collision along the eastern and southern North China margins. Tectonophysics 270 (1—2), 145—156. https://doi.org/10.1016/S0040-1951(96)00208-9.

Zhang, L.Y., Liu, Q., Zhang, C.R., et al., 2004. Restudy of pool-forming pattern of Liangjialou oilfield in Dongying sag. Oil Gas Geol. 25 (3), 253—257. https://doi.org/10.3321/j.issn:0253-9985.2004.03.003 (in Chinese).

Zhang, L.P., Wang, A.G., Jin, Z.J., 2011. Origins and fates of CO$_2$ in the Dongying Depression of the Bohai Bay Basin. Energy Explor. Exploit. 29 (3), 291—314. https://doi.org/10.1260/0144-5987.29.3.291.

Zhang, L.P., Zhao, Y.Q., Jin, Z.J., et al., 2009. Geochemical characteristics of rare earth elements in petroleum and their responses to mantle-derived fluid: an example from the Dongying Depression, East China. Energy Explor. Exploit. 27 (1), 47—68. https://doi.org/10.1260/014459809788708200.

Zhao, W.Z., Zhang, S.C., Wang, F.Y., et al., 2005. Gas accumulation from oil cracking in the eastern Tarim Basin: a case study of the YN2 gas field. Org. Geochem. 36 (12), 1602—1616. https://doi.org/10.1016/j.orggeochem.2005.08.014.

Zhu, G.Y., Jin, Q., 2003. Geochemical characteristics of two sets of excellent source rocks in Dongying Depression. Acta Sedimentol. Sin. 21 (3), 506—512. https://doi.org/10.3969/j.issn.1000-0550.2003.03.022 (in Chinese).

Zhu, D.Y., Jin, Z.J., Hu, W.X., et al., 2008. Effects of abnormally high heat stress on petroleum in reservoir—An example from the Tazhong 18 Well in the Tarim Basin. Sci. China, Ser. A D 51 (4), 515—527. https://doi.org/10.1007/s11430-008-0033-4.

Zhu, G.Y., Jin, Q., Dai, J.X., et al., 2004a. A study on periods of hydrocarbon accumulation and distribution pattern of oil and gas pools in Dongying Depression. Oil Gas Geol. 25 (2), 209—215. https://doi.org/10.3321/j.issn:0253-9985.2004.02.016 (in Chinese).

Zhu, G., Jin, Q., Zhang, S., et al., 2004b. Combination characteristics of lake facies source rock in the Shahejie Formation, Dongying Depression. ACTA GEOL SIN 78 (3), 416—427. https://doi.org/10.3321/j.issn:0001-5717.2004.03.015 (in Chinese).